

Advances in Boundary Element & Meshless Techniques XVII

Edited by
Münevver Tezer-Sezgin
Bülent Karasözen
Ferri M.H. Aliabadi

CONTENT

DRBEM for Solving Natural Convection in a Nanofluid-Filled Enclosure <i>Nagehan Alsoy-Akgün</i>	1
Particle-particle interactions in 2D MHD viscous flow <i>Selçuk Han Aydın, Antoine Sellier</i>	9
Providing Fundamental Solutions in Time Domain using Gene Expression Programming <i>Mazda Behnia, Danial Behnia, Kamran Goshtasbi Goharizi</i>	15
Meshless reconstruction of the support of a source <i>B. Bin-Mohsin, D. Lesnic</i>	23
Numerical solution to MHD pipe flow in annular-like domains <i>Canan Bozkaya, Münevver Tezer-Sezgin</i>	29
The Role of the Second Pair of Wings in Insect Flight A simple vortex approach to complex multi-wing unsteady applying problems in 2-D <i>Mitch Denda</i>	35
Performance Prediction of Wings Moving Above Free Surface <i>Ali Dogrul, Şakir Bal</i>	43
A Fast-Multipole Implementation of the Simplified Hybrid Boundary Element Method <i>Ney A. Dumont, Hélvio F. C. Peixoto</i>	51
Linear analysis of heterogeneous microstructures by the Boundary Element Method <i>Guilherme A. Ohland, Jordana F. Vieira, Matheus C. dos Santos, Gabriela R. Fernandes</i>	59
Effects of Slip Boundary Conditions on Mixed Convection flow of Nanofluids in a Lid-Driven Cavity <i>Sevin Gümğüm</i>	67
MHD Stokes flow in a smoothly constricted rectangular enclosure <i>Merve Gürbüz, Münevver Tezer-Sezgin</i>	73
Reducing the condition number of the coefficient matrix in the method of fundamental solutions for 2D Laplace equation <i>M.R. Hematiyan, M. Arezou, A. Haghghi</i>	79
Performance Prediction of 2D Foils Moving Above and Close to Free Surface <i>Ömer Kemal Kınacı, Şakir Bal</i>	85

2D Boundary element formulation for deformable particle flow in a microchannel <i>Cem Kurt, Barbaros Çetin, and Besim Baranoğlu</i>	93
Dual Reciprocity Boundary Element Solution of a System Modeling Acid-Mediated Tumor Cell Invasion <i>Gülnihal Meral</i>	99
DRBEM solution to ferrofluid flow and heat transfer in a semi-annulus enclosure in the presence of magnetic field <i>F.Sidre Oglakkaya, Canan Bozkaya</i>	107
RBF-PS Solution of the Brinkman-Forchheimer-extended Darcy model in a porous medium <i>Yasemin Öztürk, Bengisen Pekmen</i>	113
Fast numerical convolution with the Sparse Cardinal Sine Decomposition <i>Francois Alouges, Matthieu Aussal, Emile Parolin</i>	119
Fundamental three-dimensional MHD creeping flow bounded by a plane solid and motionless wall <i>Antoine Sellier</i>	125
A boundary formulation for the axisymmetric MHD slow viscous flow about a sphere translating parallel with a uniform ambient magnetic <i>Antoine Sellier, Selçuk H. Aydın</i>	131
Flow in a Square Cavity with an Obstacle under the Influence of a Non-uniform Magnetic Field <i>Pelin Şenel, Münevver Tezer-Sezgin</i>	139
A Solenoidal-Galerkin Approach for the Numerical Simulation of Flow Past a Circular Cylinder <i>Hakan I. Tarman</i>	147
Boundary integral solution of MHD pipe flow <i>M. Tezer-Sezgin, Canan Bozkaya</i>	155
POD Analysis of Drag Reduction in Turbulent Pipe Flow <i>Ozan Tuğluk, Hakan I. Tarman</i>	161
Numerical simulation of MHD duct flow problems using BEM and DGFEM approaches <i>Hamdullah Yücel, Canan Bozkaya, Münevver Tezer-Sezgin</i>	167

Meshless reconstruction of the support of a source

B. Bin-Mohsin¹ and D. Lesnic²

¹*Department of Mathematics, College of Science, King Saud University, Riyadh, Saudi Arabia, balmohsen@ksu.edu.sa*

²*Department of Applied Mathematics, University of Leeds, UK, amt5ld@maths.leeds.ac.uk*

Keywords: Inverse source problem; Method of fundamental solutions; Nonlinear optimization.

Abstract. The meshless reconstruction of the support of a three-dimensional volumetric source from a single pair of exterior boundary Cauchy data is investigated. The underlying potential satisfying the Laplace equation is sought as a discretised single-layer boundary integral representation but with sources relocated outside the solution domain, as in the method of fundamental solutions (MFS). The unknown source domain is parametrised by the radial coordinate, as a function of the spherical angles. The resulting least-squares functional estimating the gap between the measured and the computed data is minimized using the `lsqnonlin` toolbox routine in Matlab. Numerical results are presented and discussed for both exact and noisy data.

Introduction

In this paper, the aim is to reconstruct numerically in a stable and accurate manner the support of a volumetric source by employing a combined meshless technique with nonlinear optimization which have recently been developed by the authors, [1], in two-dimensions.

We consider the inverse problem of determining the support $\Omega_2 \subset \Omega \subset \mathbb{R}^3$ of an unknown volumetric source of unit intensity in the Laplace equation

$$\nabla^2 u = \chi(\Omega_2) \quad \text{in } \Omega, \quad (1)$$

where $\chi(\Omega_2)$ denotes the characteristic function of the domain Ω_2 and u is the potential. We assume that the domains Ω and Ω_2 are bounded with smooth boundaries and that $\Omega_1 := \Omega \setminus \Omega_2$ is connected. By defining

$$u =: \begin{cases} u_1 & \text{in } \Omega_1, \\ u_2 & \text{in } \Omega_2, \end{cases} \quad (2)$$

equation (1) can be rewritten as the following transmission problem:

$$\nabla^2 u_1 = 0 \quad \text{in } \Omega_1, \quad (3)$$

$$\nabla^2 u_2 = 1 \quad \text{in } \Omega_2, \quad (4)$$

$$u_1 = u_2, \quad \frac{\partial u_1}{\partial n} = \frac{\partial u_2}{\partial n} \quad \text{on } \partial\Omega_2, \quad (5)$$

where \underline{n} denotes the outward unit normal to the boundary.

We also prescribe one pair of Cauchy boundary data on $\partial\Omega$, namely,

$$u_1 = f, \quad \frac{\partial u_1}{\partial n} = g \quad \text{on } \partial\Omega. \quad (6)$$

We have the following uniqueness theorem in the class of star-shaped domains, [2].

Theorem 1. *The inverse problem (3)-(6) has at most one solution Ω_2 in the class of star-shaped domains.*

The next task is to reconstruct the source domain Ω_2 numerically. Recently, the MFS has proved, [1,3], easy to use in detecting cavities, rigid inclusions, as well as inhomogeneities in inverse geometric problems. In this paper, we investigate yet another application of the MFS to reconstruct the source domain Ω_2 from the Cauchy data (6).

In the next section we describe the MFS, as well as the nonlinear minimization proposed for reconstructing the star-shape support of the unknown source.

The method of fundamental solutions (MFS)

Prior to applying the MFS, we need to move the right-hand side inhomogeneity in (4) to the boundary conditions (5) and (6). For this, we decompose

$$u_2 = u_2^h + \frac{|\underline{x}|^2}{6}, \quad (7)$$

where the homogeneous part u_2^h satisfies

$$\nabla^2 u_2^h = 0 \quad \text{in } \Omega_2. \quad (8)$$

With the superposition (7), the transmission interface conditions (5) become

$$u_1 = u_2^h + \frac{|\underline{x}|^2}{6}, \quad \frac{\partial u_1}{\partial n} = \frac{\partial u_2^h}{\partial n} + \frac{\underline{x} \cdot \underline{n}}{3} \quad \text{on } \partial\Omega_2. \quad (9)$$

On applying the MFS we approximate the solutions u_1 and u_2^h of the Laplace equations (3) and (8) by finite linear combinations of fundamental solutions of the form, [4],

$$u_{1,2NM}(\underline{x}) = \sum_{s=1}^2 \sum_{i=1}^N \sum_{j=1}^M a_{i,j}^s G(\underline{x}, \underline{\xi}_s^{i,j}), \quad \underline{x} \in \bar{\Omega}_1, \quad (10)$$

$$u_{2,2NM}^h(\underline{x}) = \sum_{i=1}^N \sum_{j=1}^M b_{i,j} G(\underline{x}, \underline{\xi}_3^{i,j}), \quad \underline{x} \in \bar{\Omega}_2, \quad (11)$$

where $\mathbf{a} = (a_{i,j}^s)_{i=1,N,j=1,M,s=1,2}$ and $\mathbf{b} = (b_{i,j})_{i=1,N,j=1,M}$ are unknown coefficients to be determined, $(\underline{\xi}_s^{i,j})_{i=1,N,j=1,M,s=1,2}$ are source points located outside the annular domain $\bar{\Omega}_1$, $(\underline{\xi}_3^{i,j})_{i=1,N,j=1,M}$ are source points located outside the domain $\bar{\Omega}_2$, and G is the fundamental solution of the three-dimensional Laplace equation given by,

$$G(\underline{x}, \underline{\xi}) = \frac{1}{4\pi|\underline{x} - \underline{\xi}|}. \quad (12)$$

The source points $(\underline{\xi}_1^{i,j})_{i=1,N,j=1,M} \notin \bar{\Omega}$ are placed on a (fixed) dilated pseudo-boundary $\partial\Omega'$ of similar shape as $\partial\Omega$. The remaining source points $(\underline{\xi}_2^{i,j})_{i=1,N,j=1,M} \in \Omega_2$ and $(\underline{\xi}_3^{i,j})_{i=1,N,j=1,M} \notin \bar{\Omega}_2$ are placed on contraction and dilation (moving) pseudo-boundaries $\partial\Omega'_2$ and $\partial\Omega''_2$ similar to $\partial\Omega_2$ at a distance $\delta > 0$ in the inward and outward directions, respectively.

Without loss of generality, we may assume that the domain Ω is the unit sphere $B(0;1)$. We also assume that the unknown support Ω_2 is star-shaped with respect to the origin, i.e.

$$\partial\Omega_2 = \left\{ r(\theta, \phi) (\cos(\theta) \sin(\phi), \sin(\theta) \sin(\phi), \cos(\phi)) \mid \theta \in [0, 2\pi), \phi \in [0, \pi) \right\}, \quad (13)$$

where r is a smooth function with values in $(0, 1)$. In this setup of particular domains Ω and Ω_2 , the collocation and source points are uniformly distributed, as follows:

$$\begin{aligned} \underline{X}_{i,j}^1 &= (\cos(\theta_i) \sin(\phi_j), \sin(\theta_i) \sin(\phi_j), \cos(\phi_j)), \\ \underline{X}_{i,j}^2 &= r(\theta_i, \phi_j) \left(\cos(\theta_i) \sin(\phi_j), \sin(\theta_i) \sin(\phi_j), \cos(\phi_j) \right), \quad i = \overline{1, N}, j = \overline{1, M}, \end{aligned} \quad (14)$$

$$\begin{aligned} \xi_{\bar{1}}^{k,\ell} &= R \left(\cos(\bar{\theta}_k) \sin(\bar{\phi}_\ell), \sin(\bar{\theta}_k) \sin(\bar{\phi}_\ell), \cos(\bar{\phi}_\ell) \right), \quad \xi_{\bar{2}}^{k,\ell} = (1 - \delta) \underline{X}_{k,\ell}^2, \\ \xi_{\bar{3}}^{k,\ell} &= (1 + \delta) \underline{X}_{k,\ell}^2, \quad k = \overline{1, N}, \ell = \overline{1, M}, \end{aligned} \quad (15)$$

where

$$\begin{aligned} \theta_i &= 2\pi i/N, \quad i = \overline{1, N}, \quad \phi_j = \pi j/M, \quad j = \overline{1, M}, \\ \bar{\theta}_k &= 2\pi k/N, \quad k = \overline{1, N}, \quad \bar{\phi}_\ell = \pi \ell/M, \quad \ell = \overline{1, M}, \end{aligned}$$

$r_{i,j} := r(\theta_i, \phi_j)$ for $i = \overline{1, N}$, $j = \overline{1, M}$, $R > 1$ and $\delta \in (0, 1)$.

The unknown radii vector $\mathbf{r} = (r_{i,j})_{i=\overline{1, N}, j=\overline{1, M}}$, characterising the star-shaped support Ω_2 , together with the unknown MFS coefficients \mathbf{a} and \mathbf{b} , giving the approximations of the solutions u_1 and u_2 , are simultaneously determined by imposing the transmission conditions (9) and the Cauchy data (6) at the collocating points (14) in a least-squares sense. This results into minimizing the following (regularized) least-squares nonlinear objective function:

$$\begin{aligned} T(\mathbf{a}, \mathbf{b}, \mathbf{r}) &:= \left\| u_1 - f \right\|_{L^2(\partial\Omega)}^2 + \left\| \frac{u_1}{\partial n} - g^\epsilon \right\|_{L^2(\partial\Omega)}^2 + \left\| u_1 - u_2^h - \frac{|\underline{x}|^2}{6} \right\|_{L^2(\partial\Omega_2)}^2 \\ &+ \left\| \frac{\partial u_1}{\partial n} - \frac{\partial u_2^h}{\partial n} - \frac{\underline{x} \cdot \mathbf{n}}{3} \right\|_{L^2(\partial\Omega_2)}^2 + \lambda \{ \|\mathbf{a}\|^2 + \|\mathbf{b}\|^2 + \|\mathbf{r}_\theta\|^2 + \|\mathbf{r}_\phi\|^2 \}, \end{aligned} \quad (16)$$

where $\lambda \geq 0$ is a regularization parameter to be prescribed. In (16), g^ϵ is a noisy perturbation of the exact data g given by

$$g^\epsilon(\underline{X}_{i,j}^1) = (1 + \rho_{i,j} p) g(\underline{X}_{i,j}^1), \quad i = \overline{1, N}, j = \overline{1, M}, \quad (17)$$

where p represents the percentage of noise and $\rho_{i,j}$ is a pseudo-random noisy variable drawn from a uniform distribution in $[-1, 1]$ using the MATLAB \textcircled{C} command `-1+2*rand(1, NM)`, and

$$\|\mathbf{r}_\theta\|^2 = \sum_{i=2}^N \sum_{j=1}^M \left(\frac{r_{i,j} - r_{i-1,j}}{2\pi/N} \right)^2, \quad \|\mathbf{r}_\phi\|^2 = \sum_{i=1}^N \sum_{j=2}^M \left(\frac{r_{i,j} - r_{i,j-1}}{\pi/M} \right)^2. \quad (18)$$

The minimization of the functional (16) is performed using the Matlab toolbox routine `lsqnonlin` which does not require the user to provide the gradient and, in addition, it offers the option of imposing lower and upper bounds on the vector of unknowns $(\mathbf{a}, \mathbf{b}, \mathbf{r})$.

Numerical results and discussion

In all numerical experiments, the initial guess for the unknown vectors \mathbf{a} and \mathbf{b} are $\mathbf{0}$, and the initial guess for Ω_2 is a sphere centred at the origin of radius 0.7. The Matlab toolbox routine `lsqnonlin` was run iteratively until a user-specified tolerance of $XTOL = 10^{-6}$ was achieved, or until when a user-specified maximum number of iterations $MAXCAL = 1000 \times 4MN$ was reached. We have also set the simple bounds on the variable $(\mathbf{a}, \mathbf{b}, \mathbf{r})$ as the box $[-10^{10}, 10^{10}]^{2NM} \times [-10^{10}, 10^{10}]^{NM} \times (0, 1)^{NM}$. The choices of the regularization parameter λ in (16) was based on trial and error.

We consider retrieving a sphere centred at the origin of radius $R_0 = 0.5$. That is, we seek the star-shape approximation (13) for the spherical radius function

$$r(\theta, \phi) \equiv R_0 = 0.5, \quad \theta \in [0, 2\pi), \quad \phi \in [0, \pi). \quad (19)$$

We then take the analytical solutions of the equations (3)-(5) and (8) to be given by

$$u_1(r, \theta, \phi) = \frac{R_0^2}{6} - \frac{R_0^3}{3r} \quad (r, \theta, \phi) \in (R_0, 1) \times [0, 2\pi) \times [0, \pi), \quad (20)$$

$$u_2(r, \theta) = \frac{r^2}{6} - \frac{R_0^2}{3}, \quad (r, \theta, \phi) \in (R_0, 1) \times [0, 2\pi) \times [0, \pi), \quad (21)$$

$$u_2^h(r, \theta, \phi) = -\frac{R_0^2}{3}, \quad (r, \theta, \phi) \in (R_0, 1) \times [0, 2\pi) \times [0, \pi). \quad (22)$$

Based on (20), the input Cauchy data (6) are given by

$$u_1(1, \theta, \phi) = f(\theta, \phi) = \frac{R_0^2}{6} - \frac{R_0^3}{3}, \quad \theta \in [0, 2\pi), \phi \in [0, \pi), \quad (23)$$

$$\frac{\partial u_1}{\partial n}(1, \theta, \phi) = g(\theta, \phi) = \frac{R_0^3}{3}, \quad \theta \in [0, 2\pi), \phi \in [0, \pi), \quad (24)$$

and the transmission interface conditions (9) become

$$u_1(r(\theta, \phi), \theta, \phi) = u_2^h(r(\theta, \phi), \theta, \phi) + \frac{r^2(\theta, \phi)}{6}, \quad \theta \in [0, 2\pi), \phi \in [0, \pi), \quad (25)$$

$$\frac{\partial u_1}{\partial n}(r(\theta, \phi), \theta, \phi) = \frac{\partial u_2^h}{\partial n}(r(\theta, \phi), \theta, \phi) + \frac{r(\theta, \phi)}{3}, \quad \theta \in [0, 2\pi), \phi \in [0, \pi). \quad (26)$$

We solve numerically the inverse problem given by equations (3), (8), (23)-(26) to retrieve the triplet solution $(r(\theta, \phi), u_1(r, \theta, \phi), u_2^h(r, \theta, \phi))$ to compare with the analytical solutions given by equations (19), (20) and (22). Also, once u_2^h has been obtained, equation (7) yields u_2 .

Initially, we have performed several numerical runs with various values of the input MFS parameters and, for illustrative purposes, we have decided to show results only for a typical set of values $\delta = 0.5$, $R = 2$ and $N = M = 10$.

We consider first the case of exact data, i.e. $p = 0$ in equation (17). In Figure 1, we present the numerically reconstructed domain for various numbers of iterations for no noise and no regularization, as well as the exact sphere. From this figure, it can be seen that even if the input data is exact, as the number of iterations increases the numerical solution becomes more inaccurate. This is to be expected because no regularization has been imposed yet and the inverse problem under investigation is ill-posed. In order to restore stability regularization should be employed with a positive regularization parameter λ in (16).

fr
s
p
l
C
u
h
st
R
[1
M
[2
C
[3
p
14
[4
de

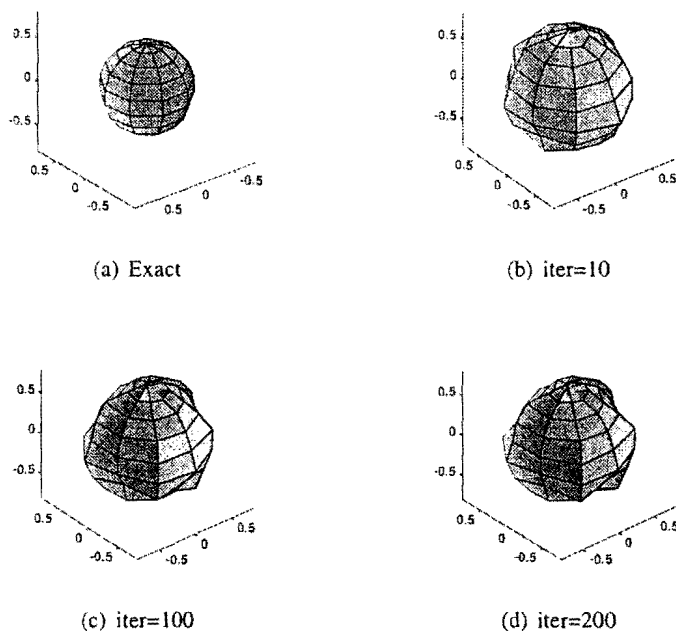


Figure 1: The reconstructed source for various numbers of iterations for no noise and no regularization.

Figure 2 shows the higher accuracy and stabilising effect that the regularization has on the retrieved shapes for values of λ between 10^{-3} and 10^{-1} .

We also perturb by a large amount of $p = 10\%$ noise the flux g , as in (17), in order to investigate the stability of the numerical solution. The numerically obtained results with various values of the regularization parameter λ after 200 iterations are shown in Figure 3. From this figure, we observe that overall λ between 10^{-3} and 10^{-2} yields accurate and stable results.

Conclusions

In this paper, an inverse geometric problem which consists of reconstructing the unknown support of a volumetric source in the three-dimensional Poisson equation from a single pair of exterior boundary Cauchy data has been investigated using the MFS. The numerical results show satisfactory reconstructions for the unknown support with reasonable stability against inverting noisy data.

References

- [1] B. Bin-Mohsin and D. Lesnic, *Reconstruction of a source domain from boundary measurements*, Applied Mathematical Modelling, submitted.
- [2] V. Isakov, S. Leung and J. Qian, *A fast local level set method for inverse gravimetry*, Communications in Computational Physics, **10**, 1044-1070 (2011).
- [3] B. Bin-Mohsin and D. Lesnic, *Determination of inner boundaries in modified Helmholtz inverse geometric problems using the method of fundamental solutions*, Mathematics and Computers in Simulation, **82**, 1445-1458 (2012).
- [4] A. Karageorghis, D. Lesnic and L. Marin, *A moving pseudo-boundary MFS for three-dimensional void detection*, Advances in Applied Mathematics and Mechanics, **5**, 510-527 (2013).

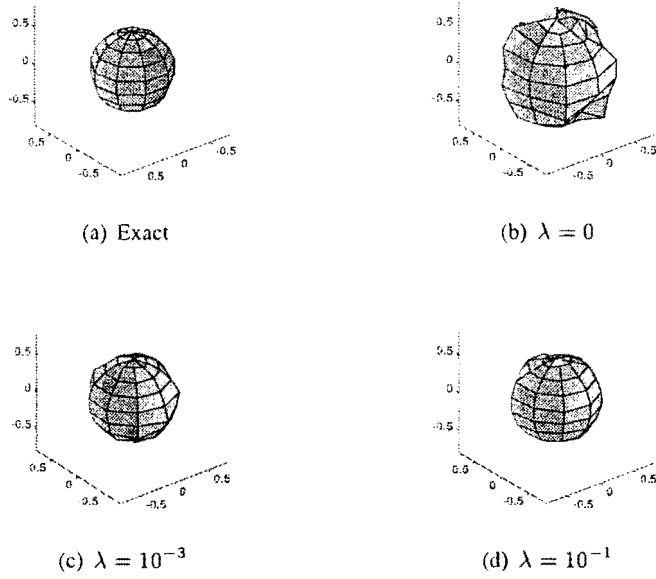


Figure 2: The reconstructed source after 200 iterations for no noise and with regularization.

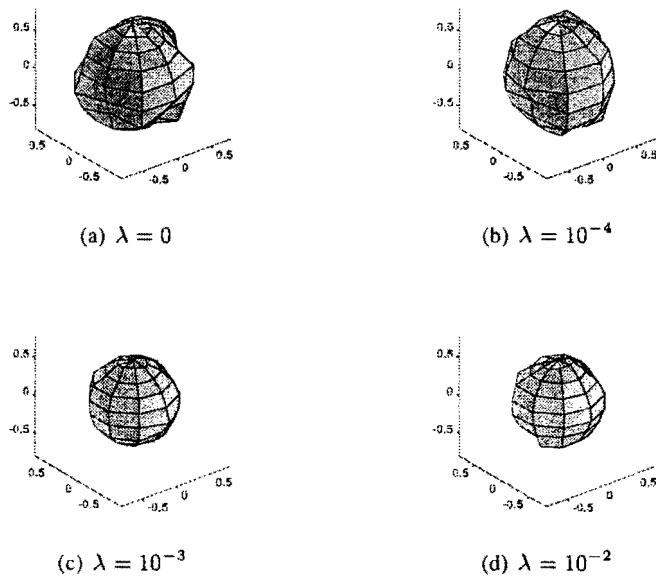


Figure 3: The reconstructed source after 200 iterations for $p = 10\%$ noise and with regularization.